Electrical Contacts to Organic Molecular Films by Metal Evaporation: Effect of Contacting Details

ARTICLE *in* THE JOURNAL OF PHYSICAL CHEMISTRY C · JANUARY 2007

Impact Factor: 4.77 · DOI: 10.1021/jp065357p

4 AUTHORS:

Hossam Haick
Technion - Israel Institute of Technology
158 PUBLICATIONS **4,435** CITATIONS
SEE PROFILE

Olivia Niitsoo
City College of New York
20 PUBLICATIONS **676** CITATIONS
SEE PROFILE

Jamal Afif Ghabboun
Bethlehem University
20 PUBLICATIONS **393** CITATIONS
SEE PROFILE

David Cahen
Weizmann Institute of Science
481 PUBLICATIONS **13,842** CITATIONS
SEE PROFILE

Electrical Contacts to Organic Molecular Films by Metal Evaporation: Effect of Contacting Details

Hossam Haick,*,† Olivia Niitsoo, Jamal Ghabboun,‡ and David Cahen*

Department of Materials and Interfaces, Weizmann Institute of Science, Rehovot 76100, Israel

Received: August 18, 2006; In Final Form: November 20, 2006

We show that electron beam evaporation of metal onto a monolayer of organic molecules can yield reproducible electrical contacts, if evaporation is indirect and the sample is on a cooled substrate. The metal contact forms without damaging even the molecules' outermost groups. In contrast, *direct* evaporation seriously damages the molecules. By comparing molecular effects on metal/molecular layer/GaAs junctions, prepared by *indirect* evaporation and by other soft contacting methods, we confirm experimentally that Au is not an optimal choice as an evaporated contact metal. We ascribe this to the ease by which Au can diffuse between molecules, something that can, apart from direct contact−substrate connections, lead to undesired and uncontrollable interfacial interactions. Such phenomena are largely absent with Pd as evaporated contact.

1. Introduction

Several developments over past decades, such as advances in molecular modification of electronic materials and in syntheses of relevant molecules,[1,2] use of scanning probe microscopies, and advanced nanofabrication methods,[3] have helped to fuel the expectations that organic molecules may become active components in future electronics.[4] However, difficulties in connecting the molecules to the macroscopic world still hinder reliable and reproducible study (and realization) of such devices;[5−7] also, contacting can damage the molecules or the substrate on which the molecules adsorbed.[8] To overcome the contacting problems, several soft contacting methods are available. These include "ready-made" contact pads (e.g., lift-off, float-on (LOFO)[9,10] and transfer printing, down to tens of nanometers, of metal pads[5,11,12]), self-assembly of colloidal particles,[13] crossed wires,[14] liquid metal (Hg),[15] spin-coating of a conductive polymer,[16,17] scanning probe microscopy,[18] and heterojunction techniques (break junction[19] and nanopores[20]). Mostly, though, these methods are limited to laboratory applications and/or to rather specific types of molecules.

Technologically, probably the most attractive method is vacuum deposition. However, generally speaking, the way it is used in microelectronics today is much too harsh for most organic molecules. In normal vacuum evaporation of metals, the atoms/clusters that reach the substrate have high temperature and kinetic energy. These factors, together with radiation, emitted from the heated source, can lead to surface modifications of the substrate.[21] If the surface is covered with molecules, those molecules will readily be damaged, while metal can penetrate through them[22−25] toward the substrate. Sputter deposition is, mostly, even more destructive.

If a metal is evaporated onto a molecule-coated metal substrate, damage is often assessed by the occurrence of electrical short circuits. If no shorts are found, this is taken to indicate the absence of damage to the molecules. Leaving aside for the moment the problem that the transition from a situation without short circuits to one that gives pure metallic conductivity (contact between two metals) is not an abrupt one, we note that the presence of shorts can very well be due to incomplete coverage, rather than to damage to the molecules. Furthermore, for semiconductor substrates, this criterion cannot be applied properly. Therefore, one is left with the challenge of how to verify that applying an electrical contact to molecules does not change the molecules.

Normal vacuum evaporation of a metal on a substrate, covered by organic molecules, is very problematic. However, since Golay first manufactured his thermal detector,[26] it has been known that the energy of the metal atoms/clusters that arrive at the surface of the substrate can be minimized by filling the evaporator chamber with an inert gas, at the expense of deposition efficiency. Cooling the substrate[27] and avoiding direct radiation of the sample,[28] by concealing it from the evaporation source or having it face away from the metal source, limits sample heating. The latter, geometric measures further minimize the kinetic energy of the atoms reaching the substrate surface.

An alternative approach is to have the molecules' terminal groups react with the impinging metal atoms, to decrease their diffusion through the molecules.[25,29] The balance between nucleation on top of the monolayer and diffusion through it depends critically on the functionality of the terminal groups and the type of the incoming metal atoms. Highly reactive metals can remain on top of the monolayer, by forming bonds with its end groups.[17,23,30−32] This approach is rather specific, though.

The resulting ambiguities in the electronic and physical characteristics of metal/monolayer interfaces, prepared by evaporation, can make interpretation of the results difficult. In view of the problem of damaging the molecules, any use of vacuum evaporated contacts necessitates finding ways to assess damage to the molecules. Here, by using a series of systematically varying molecules as such a tool, we find that details of the evaporation process can completely change the resulting device characteristics. More specifically, we show that "indirect, collision-induced, cooled electron beam evaporation" (ICICE)

* Authors for correspondence: Fax.: +972-4-8295672 (H.H.); +972-8-934138 (D.C.). E-mail: hhossam@technion.ac.il (H.H.); david.cahen@weizmann.ac.il (D.C.).

† Present address: Department of Chemical Engineering, Technion−Israel Institute of Technology, Haifa 32000, Israel.

‡ Present address: School of Chemistry, Hebrew University of Jerusalem, Israel.

10.1021/jp065357p CCC: $37.00
Published on Web 01/09/2007

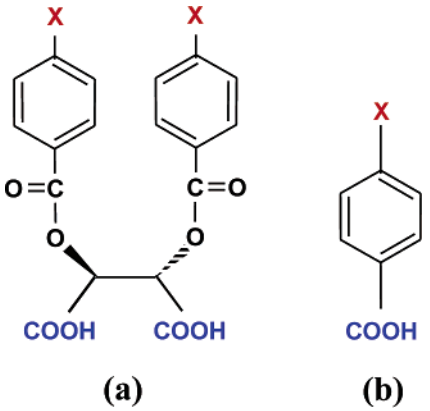

Figure 1. (a) Dicarboxylic acids (dC-X) and (b) benzoic acids (BA-X) used to modify metal/n-GaAs junctions. Changing the ligand substituents ("X" in the scheme) changes the dipole moment of the free molecules. For dC-X, X = OCH_3, CH_3, H, CN, and CF_3. For BA-X, X = OCH_3, CH_3, H, CN, CF_3, $N(CH_3)_2$, F, Br, and NO_2.

does far less damage than "direct evaporation under cryogenic cooling" (DEUCC) and yields reproducible results, especially when Pd is used for contacting. Our conclusions are based on experiments with molecular monolayers that are chemically bound to a GaAs substrate, the use of Au and Pd as evaporated contacts, and comparison of our results with earlier ones obtained by another contacting method, LOFO.[9] Preliminary reports on our study can be found in refs 33−35.

2. Experimental Section

Semiconductor/metal junctions were prepared and characterized as follows:

2.1. Substrate Pretreatment. n-GaAs(100) (Si doped, 10^{18} cm^{-3}) substrates were cleaned by immersing sequentially in hot solutions of acetone, methanol, and chloroform for 10 min each, followed by ozone oxidation for 10 min in a UVOCs apparatus. The oxide was removed by a 50 s dip in NH_4OH:H_2O (1:10 v/v) solution, after which the samples were briefly immersed (3 s) in 18 MΩ deionized water, in acetonitrile (ACN), and immediately placed in the adsorption solutions.

2.2. Ligand Adsorption. GaAs surfaces were modified by binding molecules of dicarboxylic (dC-X) acids with varying substituent groups (X = OCH_3, CH_3, H, CN, or CF_3; cf. Figure 1a) onto them.[36] This was achieved by adsorbing the molecules overnight from 2.5 mM solution in ACN onto the substrate. The surfaces were then rinsed in clean ACN for 30 s and dried with pure N_2. Adsorption of the molecules, between ∼0.5 and ∼0.9 monolayer (ML), was verified by Fourier transform infrared (FTIR) spectroscopy, contact potential difference (CPD), ellipsometry, and water contact angle measurements.[36,37] Molecular coverage on GaAs is generally 70−80% for dC-X molecules. The dC-X thickness values, extracted from the capacitance data,[38] are 0.64−0.71 nm.[9,39,40]

For specific experiments, when there was a need for GaAs surfaces covered with as dense a molecular monolayer as possible, rather than the partial dC-X monolayer, the substrates were directly immersed in ACN solution that contained both 2.5 mM dC-X and 0.83 mM benzoic acid (BA-X; X = OCH_3, CH_3, H, CN, CF_3, $N(CH_3)_2$, F, Br, or NO_2; cf. Figure 1b). BA-X adsorbs onto GaAs through its carboxylic group, as dC-X does, but, because it is much smaller, adding it provides extra coverage. Molecular coverage on GaAs is generally 80−85% for BA-X molecules. The mixed monolayers were characterized by the same techniques as those used for those with only dC-X derivatives.

2.3. Contact Potential Difference (CPD). CPD was measured in ambient conditions (293 K, 40% relative humidity), with a home-built system, based on a Besocke Kelvin probe, to determine the electrical potential of contact-free surfaces relative to that of a (Au) reference. For molecules on a semiconductor surface the CPD reflects the work function of the surface, i.e., the electron affinity, χ, plus the energy difference between the conduction band minimum and the Fermi level. The work function will vary with the potential drop, ΔV, over a surface dipole layer, which is a function of the molecule's dipole moment, μ,[41] according to[42−44]

$$\Delta V = \frac{N\mu \cos\theta}{\epsilon\epsilon_o} \quad (1)$$

Here, N is the molecular density of the different derivatives; θ is the average tilt of molecules relative to the surface normal; ϵ is the effective dielectric constant of the molecular film (including any depolarization effects[45]); ϵ_o is the permittivity of free space.[44] The dipole is defined as positive if its positive pole is closest to the substrate. This also defines the sign of ΔV.

The energies of the semiconductor bands at the surface are normally shifted with respect to the Fermi level, compared to their value in the bulk, due to surface charges. This difference is the band bending (BB), which is taken positive for an n-type semiconductor with a depletion layer. These surface charges can be neutralized and, thus, the band bending can be eliminated, by illumination with saturating supra-band-gap illumination. The resulting CPD value, CPD_L, reflects, for an n-type semiconductor such as the GaAs used in this study, the electron affinity, χ, to within the energy difference between the Fermi level and the conduction band, which is negligible in our case as the GaAs is virtually degenerate. The difference between CPD_L and that obtained in the dark is the surface photovoltage (SPV). For conversion of the experimental CPD values to work functions and electron affinities, we took the Au work function as 5.0 eV.

2.4. Top (Metal) Contacts. Deposition of metal (Au or Pd) contacts was started immediately after completion of the adsorption process, using either of two main evaporation modes: indirect, collision-induced, cooled evaporation (ICICE) or direct evaporation under cryogenic cooling (DEUCC). In indirect evaporation (cf. Figure 2) the process was performed as follows:

(I) The modified substrates were placed on a specially built sample holder. The front side of the holder, on which the samples were placed, consisted of a perforated plate (with 9 holes/cm^2, 0.5 mm diameter), made of oxidation-resistant Cu alloy. The back side, which faced the crucible during indirect evaporation, was covered by a 3 mm thick thermally insulating layer of Teflon-sandwiched layers of Ti (200 nm) and Al_2O_3 (1500 nm). These layers assured that irradiation emitted from the crucible did not heat the samples from the back side, through the holes in the holder (the holes served as bases for the clips used to hold the shadow mask, described in step II).

(II) Shadow masks were put on top of the samples and held there by thin (1.54 mm^2 contact area), but mechanically stable clips. The masks, made from 0.2 mm thick Ni, contained 0.5 mm diameter holes, spaced 0.7 mm apart (Suron A.C.A. Ltd., Israel).

(III) The sample holder was attached to a cooling finger, attached to the upper cover of the evaporator's vacuum chamber (cf. Figure 2, cooling finger 1). The front side of the sample holder (to which the samples and shadow mask were attached)

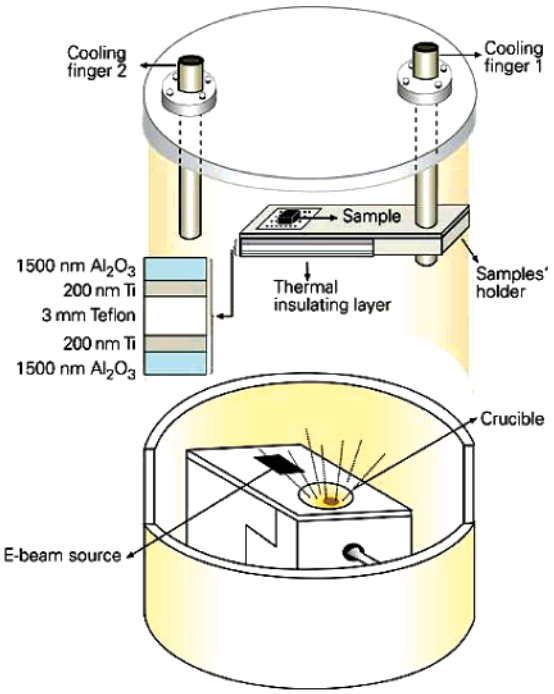

Figure 2. Cross-sectional schematic view of the vacuum chamber used in indirect, collision-induced, cooled evaporation (ICICE). Samples were placed on an oxide-free Cu holder and faced *away* from the crucible. Evaporation was started after a base vacuum pressure was reached, then the chamber was filled with low pressure of argon, and the sample holder was cooled to 150−200 K. The difference with direct evaporation under cryogenic cooling (DEUCC) is that there the samples, on a sample holder cooled to 90 K, *face* the metal crucible and that evaporation itself occurs at the base vacuum pressure, without the presence of Ar.

faced away from the crucible, so that it was ∼30 cm above the crucible and 50°−60° relative to the crucible's center (Figure 2).

(IV) After a base vacuum pressure of 2×10^{-6}−8×10^{-7} mbar was reached, liquid N_2 was introduced in a cooling finger (cooling finger 2 in Figure 2), with a relatively large surface area (400−500 cm^2), some 20 cm from cooling finger 1. Cooling finger 2, which was colder than cold finger 1 (150−200 K; vide infra), served to keep condensation products from accumulating on the sample. The temperature of cooling finger 2 was 77 K, for at least 60 min before starting evaporation and then kept at this temperature during evaporation.

(V) The chamber was filled with $(2.0-2.5) \times 10^{-3}$ mbar pressure of Ar, via a needle valve.

(VI) The sample holder was cooled to 150−200 K, by a mixture of liquid and gaseous N_2, through cooling finger 1.

(VII) Metal evaporation was at a rate of 0.01−0.03 nm/s, except for the samples used for scanning electron microscopy (SEM) and atomic force microscopy (AFM) experiments, where the rate was at most 0.01 nm/s. The thickness was probed by an FTM5 plano-convex quartz crystal thickness monitor (14 mm in diameter, 0.3 mm thick, 6 MHz nominal frequency) that was placed next to the sample and *faced* the crucible. For the SEM and AFM samples the thickness monitor *faced away* from the crucible.

(VIII) The thickness of the evaporated metal was correlated with the required effective thickness by separate calibration experiments, in which this monitor was put in place of the sample holder. This is necessary since only metal atoms that scatter off Ar atoms reach the sample. The efficiency of the evaporation process (i.e., the ratio between evaporated metal and deposited metal) is 6−8% and ∼30% for Au and Pd, respectively, with effective deposition rates of $(0.6-2) \times 10^{-3}$ nm/s and $(3-9) \times 10^{-3}$ nm/s.

TABLE 1: Molecular Dipole Moments of dC-X Molecules Adsorbed on GaAs(100) Surfaces, from Ref 39

molecule	dipole moment (D)
dC-OCH_3	−3.9
dC-CH_3	−2.9
dC-H	−2.0
dC-CF_3	+2.1
dC-CN	+3.7

(IX) After evaporation, the samples were allowed to warm to room temperature in the Ar atmosphere, before the vacuum was broken.

For direct evaporation, the samples were held on the sample holder as described in steps I and II of the indirect evaporation process described above, but now they faced the crucible. Changing the holder position between 10 and 40 cm above the crucible did not affect the results significantly. Direct evaporation was done at a base pressure of 2×10^{-5}−7×10^{-7} mbar and at rates of 0.05−0.25 nm/s, while cooling the samples cryogenically (90 K). Unless otherwise stated, all directly evaporated junctions reported here were prepared at a pressure of 2×10^{-6} mbar, a rate of 0.15 nm/s, and a substrate-to-crucible distance of 25 cm. In the following direct and indirect evaporation will refer to DEUCC and ICICE, respectively, unless specifically noted otherwise.

The procedure for lift-off, float-on contacting was as described elsewhere (the so-called "fast LOFO" variant was used).[9]

2.5. Quantum Chemical Calculations. The calculated dipole moments of the free dC-X molecules, bound to the GaAs surface, are shown in Table 1. They were taken from ref 39, where they were calculated with the Gaussian 03 package,[46] using the PBE1PBE/6-31+G(d,p) method. While these values differ slightly from those of the free molecules that we used in our earlier work,[33−35,47−50] the trends are very similar.

2.6. Scanning Electron Microscopy (SEM). A Leo Ultra microscope at 2 kV accelerating voltage was used to inspect the substrates and the metal surfaces.

2.7. Atomic Force Microscopy (AFM) was done in the semicontact mode, using a Digital Instruments Nanoscope III microscope with standard silicon tips (Olympus OMCL-AC160TS). Both topology and phase images were recorded. Phase imaging is an imaging method that is complementary to topographic imaging, done with the semicontact technique, known as the tapping mode. The phase and semicontact images are acquired simultaneously, but the topographic image is derived from change in the oscillation amplitude of the tip while the phase image is derived from change in the time response (phase lag) of the oscillating tip. If an area of different viscoelasticity or adhesion is scanned, the time response of the oscillating tip changes as the tip sticks to the surface and a relative difference is detected while the topographical information remains unchanged. This allows distinguishing between regions of high and low surface adhesion or hardness.

2.8. Time-of-Flight Secondary-Ion Mass Spectrometry (TOF SIMS) was used to probe the organic molecules beneath the ∼30 nm thick metal contacts. The experiments were done with a PHI TRIF-II spectrometer. Samples were bombarded with a 1 keV Cs^+ pulsed ion beam to remove atoms from the outermost atomic surface layer over an area of 500 × 500 μm, and with a 15 keV Ga^+ beam over a raster size of 50 × 50 μm (located in the middle of the 500 × 500 μm domain "sputtered" by the 1 keV Cs^+) to obtain elemental and molecular chemical information about the surface. To be able to draw conclusions

about the relative concentrations of the different parts of the organic molecules (cf. Table 2) beneath the metal contacts, the peak profiles of the samples were integrated numerically and compared to those without metal contacts.

2.9. X-ray Photoelectron Spectroscopy (XPS). XPS surface analyses were performed, using the Al Kα X-ray source of a Kratos Axis-HS instrument, on structures with very thin (~0.5−1 nm), partial metal films, which were prepared ex situ. Measurements were taken with electron takeoff angles between 10° and 80°. Ten samples were introduced simultaneously in the spectrometer within 3 h of finishing the contacting process.

2.10. Electrical Measurements. Current−voltage (*I*−*V*) characteristics were recorded with an HP4155 semiconductor parameter analyzer between −1 and +1 V in steps of 0.01 V at room temperature. The back (Ohmic) contact to the semiconductor was made by spreading an In−Ga eutectic, and the Au pad, contacted by a micromanipulator (Karl Suss). At positive bias the semiconductor was positive with respect to the tip. The results were analyzed according to the thermionic emission model.[51] In this model electron transport is viewed as a thermally activated process, where only electrons with sufficient thermal energy (in the "Boltzmann tail") can surmount the electrostatic Schottky barrier in the semiconductor, if such a barrier formed upon metal/semiconductor contact formation.

C−*V* measurements on Pd ICICE structures were recorded in vacuum (2×10^{-4} mbar) at room temperature with an HP 4194 impedance analyzer between −0.8 and 0.8 V dc bias at 1 MHz. The data were analyzed according to an equivalent circuit of three capacitors in series, following a procedure similar to that described in ref 38. Further details are given in ref 33.

3. Results

To assess how molecules are affected if a relatively thick (~30 nm), continuous layer of metal is evaporated on top of them, we used molecules whose functionality (polarity of the molecules, quantified by dipole moment, in our case) is determined by an exposed functional group. In the adsorbed molecules this group is the one most exposed to the outside, i.e., also to the metal atoms and clusters that land on the surface, during evaporation. Therefore, any damage to the molecule will immediately be expressed as a change in its functionality. Within the series of dC-X polar molecules that we use (cf. Figure 1a), the molecular dipole moment varies systematically. Earlier we showed that these molecules change the surface potential of the substrate onto which they are deposited in the same systematic fashion as the variation of their dipole moment.[36,49] If these molecules are placed at the interface between a metal and a semiconductor, then, if they are not damaged by the contacting, they exert this same systematic influence on the effective barrier height for current transport across the metal/semiconductor junction.[33−35,48−50] We also showed that polar molecules can control charge transport across a metal/semiconductor interface, even as a partial film at the interface.[35,52] This behavior is due to the long-range electrostatic effect of (molecular) dipole domains, which also affects the electrostatic potential of semiconductor regions under the film's pinholes and, with it, electronic transport through the pinholes. In these junctions tunneling *through* the molecules is negligible compared to transport via the pinholes.[35,52] For our purposes the important issue is that only if the molecules' exposed, functional groups remain intact can we expect that the current−voltage (*I*−*V*) characteristics of the resulting junctions will vary systematically with the change in those functional groups.

Before metal contacting, the free surface potential, given as the contact potential difference under saturating, supra-band-gap illumination, CPD_L, of the molecularly modified GaAs surfaces, was measured and found to vary with the free molecules' dipole moment (Figure 3). CPD_L presents the electrostatic potential, built up between an (external, noncontacting) Au electrode and the derivatized n-GaAs surfaces, as measured under saturating illumination.[53] Since CPD_L yields values that are averaged over the surface, it varies with and reflects surface coverage. Therefore, when we will later look at differences between junctions made on surfaces, modified by the different molecules, we will plot the barrier heights vs CPD_L rather than vs free molecule dipole, to eliminate the variations due to differences in coverage.

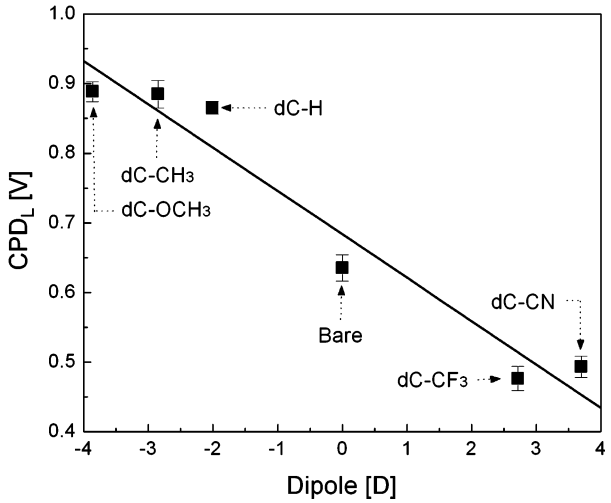

Figure 3. Contact potential difference under illumination, CPD_L, of n-GaAs as a function of the dipole moment of the substituted dicarboxylic acids adsorbed on it (from Table 1 and ref 39).

If we evaporate a Pd or Au contact indirectly on the modified surfaces and measure the current−voltage (*I*−*V*) characteristics of the resulting junctions, we see a clear effect of the molecules, by comparing them to those of the bare (Pd/n-GaAs or Au/n-GaAs) junction (Figure 4). Surprisingly, the systematic effects of the molecules for junctions made with Pd and with Au are opposite to each other. While molecules with a negative dipole (dC-OCH_3, dC-CH_3, dC-H; cf. Table 1) increase the current in Pd/dC-X/n-GaAs structures, according to their magnitude, they decrease it in Au/dC-X/n-GaAs structures, and vice versa for positive dipoles (dC-CN and dC-CF_3; cf. Table 1).[54]

Irrespective of the different *I*−*V* trends of molecularly modified junctions, which we will discuss in section 4.4, the systematic molecular effects shown in Figure 4 suggest that indirect evaporation provides contacts that do no damage to the organic molecules and their functional groups, or do so little damage that the systematic variation between molecules is preserved. Also, these results suggest that no strong interactions occur (and no chemical bonds were formed) between the metal and the terminal groups, because we would expect such interactions to disturb the systematic way in which the functional groups influence the *I*−*V* curves.

Using direct evaporation to deposit the metal contacts onto the molecularly modified surfaces did not yield any systematic correlation between the *I*−*V* characteristics of the resulting junctions and the molecular dipoles with either Pd or Au (Figure 5). In these junctions, the currents are much higher than for the junctions prepared by indirect evaporation. *I*−*V* characteristics of the directly evaporated junctions are also more symmetric than those obtained for junctions prepared by indirect evaporation; i.e., there is little if any current rectification. For the Au/n-GaAs junctions some effect of the molecules is seen, namely

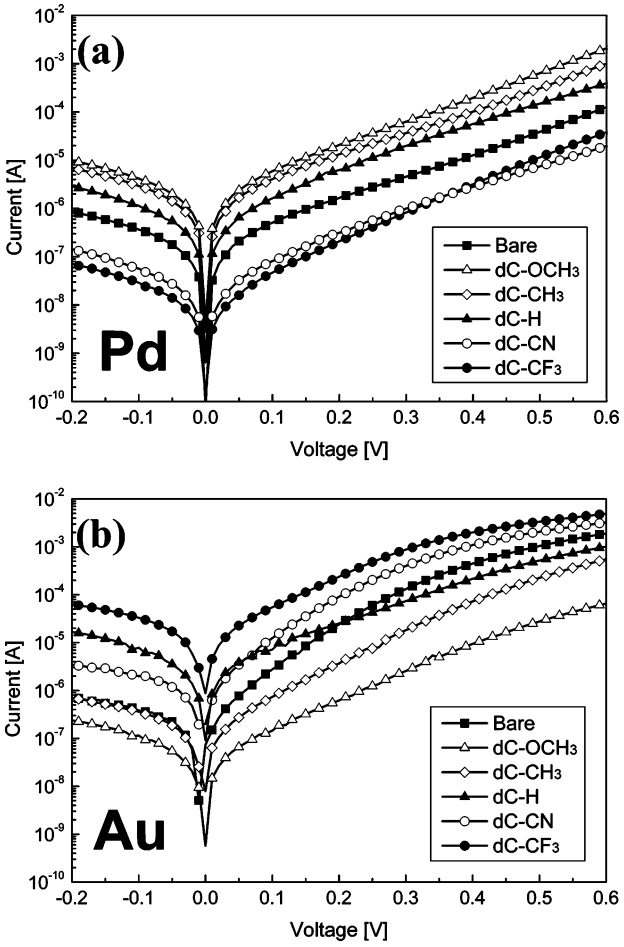

Figure 4. Typical ln(current)−voltage, ln(I)−V, curves for bare and molecularly modified metal/n-GaAs junctions contacted by indirectly evaporated (a) Pd and (b) Au. The curves are for the bare interface and for molecularly modified interfaces with different substituents on the dicarboxylic acid (dC-X) ligands: dC-OCH_3, dC-CH_3, dC-H, dC-CN, and dC-CF_3. The data were averaged geometrically over 10−15 measured diodes (0.2 mm^2 area) and are presented as a single curve for each voltage. Five or more samples of each given type were measured. The points/symbols are inserted to distinguish between the curves. Actual data were taken at 0.01 V intervals.

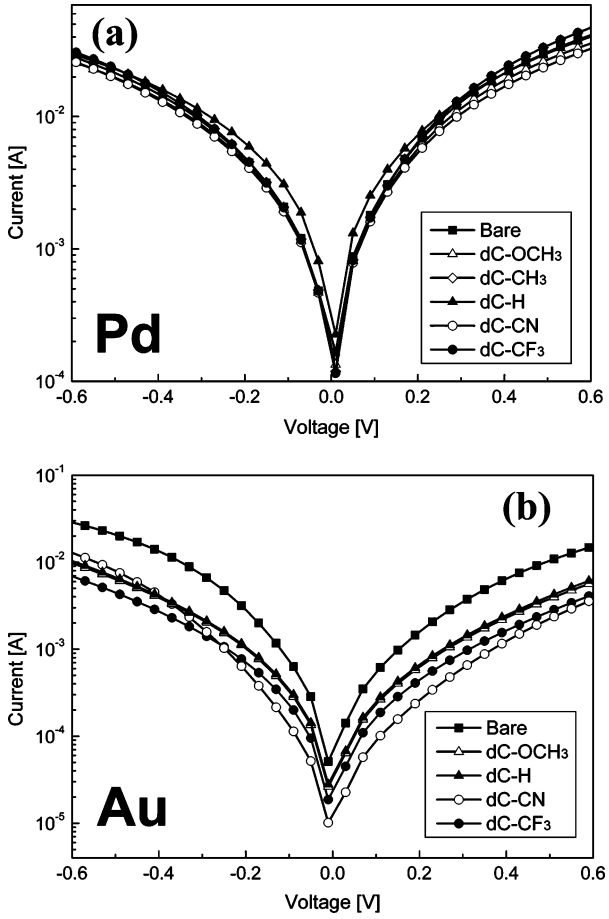

Figure 5. As Figure 4, but for junctions prepared by direct evaporation (DEUCC).

a noticeable current reduction compared to the junction without molecules at the interface. No such effect is seen for the Pd/dC-X/n-GaAs junctions.

From the ln(I)−V characteristics of the different junctions, effective barrier heights (BHs) were derived, by fitting the curves, between 0.06 and 0.4 V, to the Schottky thermionic emission model, given by[51]

$$I = SA^*T^2 \exp\left(-\frac{q\phi_b}{k_BT}\right)\left[\exp\left(\frac{qV}{nk_BT}\right) - 1\right] \qquad (2)$$

where I is the measured current, V is the applied bias, S is the actual geometric area of the diode (=0.2 mm^2), A^* is the theoretical Richardson constant (=8.6 $A \cdot cm^{-2} \cdot K^{-2}$ for n-GaAs), q is the fundamental charge, n is the ideality factor, k_B is the Boltzmann constant, and T is the temperature in kelvin. Plotting the extracted BHs versus the experimentally observed CPD_L shows a clear difference between direct and indirect evaporated contacts, as well as between indirectly evaporated Pd and Au contacts (Figure 6). For junctions prepared by indirect evaporation, the BH values correlate linearly with CPD_L, but, as noted already, with *opposite* trends. While positive dipoles increase the BHs for Pd−ICICE junctions, relative to the bare one, they

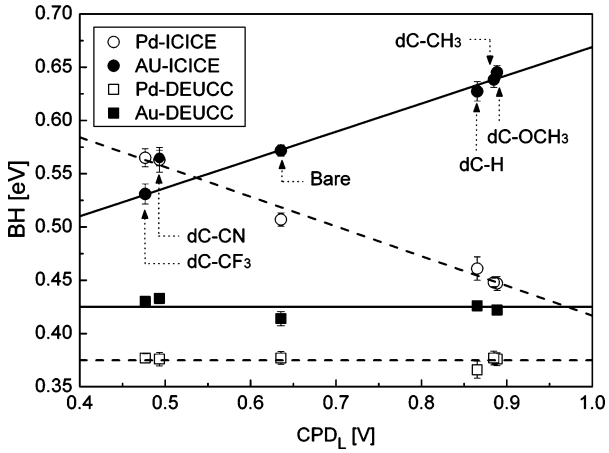

Figure 6. Dependence of barrier height (BH), at metal (Pd or Au)/dC-X/n-GaAs junctions contacted by indirect and direct evaporation, on CPD_L for surfaces modified by the series of dicarboxylic acids. BH values for indirectly evaporated junctions were calculated using the 0.06−0.40 V range of data, whereas those for directly evaporated ones were calculated using the 0.06−0.25 V range of data. The CPD_L data (and error bars) are given in Table 3 and are the same for the four plots.

decrease them for Au−ICICE ones, and vice versa for negative dipoles. The extent of the molecular effects, in terms of maximum difference between the highest and the lowest BHs, extracted for a given junction, was comparable (0.12 eV). The values of the "ideality factor", n, for junctions contacted with Au−ICICE (n = 3.3−4.4) were even higher than those for junctions contacted with Pd−ICICE (n = 2.4−3.3). Such high

TABLE 2: Relative Change in Concentrations of Different Chemical Groups at the Metal/dC-CF_3/GaAs Interface, C_R,[a] from TOF SIMS

	C_R, indirect evaporation (%)[b]		C_R, direct evaporation (%)[b]	
	Pd	Au	Pd	Au
COO	-2 ± 0.5	-5.5 ± 0.5	-59 ± 4	-79.5 ± 6.5
CF_3	-6.5 ± 0.5	-9.5 ± 1	-89.5 ± 3	-81.5 ± 5.5
CF_x ($x = 1, 2$)[c,d]	$+1 \pm 0.2$	$+2 \pm 0.5$	$+21 \pm 3$	$+22 \pm 4$
F	$+5.5 \pm 1$	$+18 \pm 1.5$	$+149 \pm 8$	$+8 \pm 2$
CC	-7 ± 1	-5.0 ± 0.53	-29.5 ± 3	-7.5 ± 1

[a] Except for the CF_x case (cf. footnote *c*), $C_R = (C_{metal/dC\text{-}CF_3/GaAs} - C_{dC\text{-}CF_3/GaAs})/C_{dC\text{-}CF_3/GaAs}$, where $C_{metal/dC\text{-}CF_3/GaAs}$ and $C_{dC\text{-}CF_3/GaAs}$ are the concentrations of a given chemical group in the metal/dC-CF_3/GaAs junction and on the contact-free dC-CF_3/GaAs surface, respectively. $C_R < 0$ indicates changes due to decomposition of chemical groups. [b] Induced damage of molecules during metal evaporation starts, sequentially, from the functional group (CF_3 here), continues to the molecule backbone (which we sense as C−C), and ends at the binding group to the surface (sensed as COO). We use the term "complete/total damage" by considering samples with the highest C_R of the COO groups, and the term "partial damage" for the samples that have the least damaged CF_3 groups. [c] No signals of CF_x ($x = 1, 2$) were obtained in the contact-free dC-CF_3/GaAs surface. Since that is so, the changes in the concentration of these groups (i.e., those presented in the table) were taken relative to the concentration of the CF_3 groups in the contact-free surfaces. [d] The signal/noise ratio in these measurements makes it impossible to distinguish between CF− and CF_2− species in metal/dC-CF_3/GaAs junctions.

n values suggest that the junctions are inhomogeneous and that those with Au are more so than those with Pd.[52,55,56]

In contrast to these results, no clear BH−CPD_L dependence is found for the series of junctions prepared by direct evaporation of Pd or Au. The changes in BHs, relative to the bare junction, are within the experimental error for Pd. For junctions with directly evaporated Au contacts these changes are very much smaller (a few tens of millielectronvolts) than the clear systematic effects seen in junctions prepared with indirectly evaporated Au, and are all in the same direction with respect to the BH for the bare junction.

Preservation of the effect of the molecular function after metal contact deposition, as seen after indirect evaporation, is prima facie evidence for damage-free contacting. This conclusion does not, however, explain the differences between junctions prepared by indirect evaporation of Pd and Au.

To understand those differences and to see under which conditions the metals damage the molecules, additional analyses were performed. In these analyses representative samples of contact-free dC-CF_3/GaAs surfaces and of Pd/dC-CF_3/GaAs and Au/dC-CF_3/GaAs junctions, contacted by either indirect or direct metal evaporation, were characterized by TOF SIMS.[57] The CF_3 derivatives were chosen to facilitate these analyses. For our purposes, TOF SIMS has some advantages over more common surface analyses, including ultrahigh sensitivity to surface layers (one atomic layer), detection of atomic concentrations as low as 10 ppm, and detection and analysis of organics and inorganics with submicrometer lateral resolution. In the TOF SIMS experiments the junctions were bombarded with a 1 keV pulsed ion beam to remove atoms from the *outermost* atomic surface layer. At each step, elemental and molecular species from the surface were detected, including C−C ($m/z = 24$), COO ($m/z = 44$), CF_3 ($m/z = 69$), and F ($m/z = 19$) groups that relate to different parts of the dC-CF_3 molecules.

Signals related to different chemical groups of dC-CF_3 molecules were detected after a layer of metal of roughly the contact thickness (~30 nm) was sputtered off. Table 2 summarizes the relative changes in concentrations of different chemical groups at the metal/dC-CF_3/GaAs interface, probed by TOF SIMS. The results show a lower concentration of COO binding groups, CF_3 functional groups, and C−C species at metal/dC-CF_3/GaAs junctions, than on contact-free dC-CF_3/GaAs surfaces. Irrespective of the metal type, in junctions contacted by indirect evaporation the results show higher concentrations of COO and CF_3 groups than in those contacted by direct evaporation, while the concentrations of carbon species are roughly comparable. The situation is opposite for F species, as junctions contacted by direct evaporation show higher F concentrations than those contacted by indirect evaporation. Neither H_2O nor Ar was detected by TOF SIMS.

From analyses of these results we find that indirect evaporation of Pd preserves almost all the COO binding groups, and ~6% of the CF_3 groups are damaged. About 1% of all the CF_3 groups (viz., the CF_3 groups in contact-free dC-CF_3 surfaces) decomposed to charged CF_x ($x = 1, 2$) species, and ~5% decomposed to smaller atomic F species (cf. Table 2, footnote *b*). For indirectly evaporated Au, the results show a similar effect on the binding groups as for Pd, and ~9% damage to the CF_3 groups, of which nearly half decomposed to charged CF_x ($x = 1, 2$) species and the rest to smaller atomic, F, ones.

For directly evaporated Pd and Au junctions the calculations show that close to 60% and 80% of the molecules, respectively, are seriously damaged. This includes decomposition of the functional groups, backbone, and binding groups as well. The remaining part includes partially damaged as well as undamaged molecules. For directly evaporated Pd a stronger effect on the functional groups is seen than for Au. Complementary calculations, based on mass transport equations, show that close to 10% and 15% of the decomposed CF_3 groups, in directly evaporated Pd and Au junctions, respectively, were altogether removed from the junction (not shown in Table 2).

To verify that the molecules remained undamaged below the indirectly evaporated contacts, we evaluated the monolayer thickness below these contacts by capacitance−voltage ($C-V$) measurements, for junctions that showed clear molecular effects. The experimental data on representative Pd/dC-X/n-GaAs junctions prepared by indirect evaporation were analyzed, using an equivalent circuit of three capacitors in series, each with its associated resistor, to account for the capacitance of the space charge layer of the semiconductor, of the organic layer, and of the top contact. The monolayer thickness values, extracted from the capacitance data,[38] were compared to those calculated by density functional theory (DFT), which, assuming a $50° \pm 5°$ tilt angle of the molecules, relative to the surface normal, are 0.64−0.71 nm.[9,39,40] These values agree well with the *average* thickness of the different molecular monolayers, extracted from the $C-V$ data, of 0.68 ± 0.05 nm.[33] This agreement supports the presence of undamaged molecules below the indirectly evaporated metal contact. Even the relatively large difference between the thickness of the dC-CH_3 monolayer derived from the experimental $C-V$ data (0.78 ± 0.09 nm) and the thickness calculated by DFT (0.64 ± 0.06 nm) is within the error, which,

for the DFT-derived values, arises from the uncertainty in the tilt angle of the molecules adsorbed on the substrate.[33]

4. Discussion

4.1. Why Use Indirect Evaporation? Making electrical contacts by metal evaporation relies on vaporizing the metal by heating it to sufficiently high temperatures to make it volatile and recondensing it onto a cooler substrate. Once the metal is evaporated, its vapor undergoes collisions with the surrounding gas molecules inside the evaporation chamber. As a result, a fraction is scattered within a given distance during their transfer through the ambient gas. For unlike molecules, the mean free path, λ (i.e., the average distance traveled before collision with another molecule), of projectile i in a background gas of species j at the same temperature is given by[58]

$$\lambda_{ij} = \left[\left(1 + \frac{M_i}{M_j}\right)^{1/2} n_j \sigma_{ij}\right]^{-1} \quad (3)$$

where M_i and M_j are the molecular masses for species i and j, respectively, n_j is the volume density of species j, and σ_{ij} is the effective molecular collision cross section, related to the molecular diameter, D, and given by

$$\sigma_{ij} = (1/4)\pi(D_i + D_j)^2 \quad (4)$$

Based on eqs 3 and 4, the mean free path of Au (or Pd) in a $10^{-4}-10^{-6}$ mbar vacuum is ~80−8000 cm. Therefore, placing the samples at a distance of (at least) 80 cm from the metal source and evaporating in a vacuum of 10^{-4} mbar should decrease the kinetic energy of the atoms and clusters that reach the sample surface. In this way damage to the samples should be reduced by assuring more "gentle" deposition of the evaporated atoms and clusters. However, evaporation under such vacuum conditions involves surface contamination, which, by itself, can disturb the (electrical) characteristics of the resulting interface. While contamination is almost excluded if evaporation is performed in a vacuum better than 10^{-6} mbar,[59] this necessitates placing the samples at unrealistically large distances from the crucible. In addition, one needs to consider that radiation emitted from the metal source can arrive at the sample surface and affect the substrate and/or the molecules adsorbed on it.[21,60]

Introducing an inert gas into the chamber after achieving a base vacuum pressure $<10^{-6}$ mbar, will decrease the total vacuum in the chamber while keeping the concentration level of the contaminants similar to that in the system with the high base vacuum. Introducing Ar as the inert gas, to reduce the vacuum by bringing the pressure in the chamber to ~10^{-3} mbar, as done here, decreases the mean free path of the evaporated atoms/clusters to ca. 11 cm, which is much less than the distance between the sample and the metal source (~30 cm). Therefore, only metal atoms/clusters that are scattered several times by Ar atoms can reach the sample surface. As a result, most of the metal atoms/clusters reach the sample surface with low kinetic energy. Since the sticking coefficient of Au on the stainless steel walls of the evaporation chamber (~1) is much higher than that of Ar (0−0.1),[61] we neglect scattering of Au from walls.[62] For direct evaporation, the temperature of *evaporated* atoms and clusters seems to play less of a role in damaging the molecules than their kinetic energy. In complementary experiments the temperature of the evaporated species on the sample surface was measured to be 318−328 K, significantly lower than the 363−383 K temperatures required to induce irreversible defects in monolayers of molecules with carboxylate binding groups.[63] However, radiation emitted from the crucible can affect the semiconductor surface and/or the molecules,[21] as mentioned in the Introduction. This necessitates shielding the sample from this radiation. We found that, if the samples face away from the crucible, radiation can affect them (via heating the sample holder) and that even a thermally insulating layer on the back side of the (otherwise thermally conductive) sample holder did not prevent sample heating. Thus, in prolonged evaporation runs (>1 h), as is often required for indirect evaporation because of the low evaporation rate, we found a temperature increase of the sample holder up to 450 K, i.e., above the temperature that can induce irreversible damage/defects for most of the organic monolayers.[64,65] This is the reason that forced cooling was added to keep the sample holder at 150−200 K during indirect evaporation.

4.2. Effect of Contacting Method. The results presented in Figures 4 and 6 indicate that *indirect* evaporation of metal on a cooled substrate minimizes damage to molecules sufficiently so that molecular trends are preserved in the resulting devices. Furthermore, the results are consistent with the absence of chemical bond formation between the metal and the termination groups, as that is expected to disturb the systematic effects of the exposed functional groups.

In contrast to indirect evaporation, the high leakage currents and inferior rectifying behavior observed in the junctions prepared by direct evaporation (Figure 5) indicate that the metal atoms and radiation emitted from the crucible damage the GaAs surface. This radiation, which includes X-rays (as a result of electron−metal interaction), stray electrons from the electron-beam source, and electrons backscattered from the molten metal target, can be intense enough to lead to compositional changes of the GaAs surface.[60] Therefore, it is clear that molecules, adsorbed on that surface, will be damaged as well.

As shown in Figure 5, cooling the substrate cryogenically, as in direct evaporation, does not preserve the systematic effect of changing the organic molecules. The TOF SIMS analyses show that direct evaporation leaves only a small fraction of the molecules intact. The remainder is either completely damaged (decomposition of the binding group, the skeleton, and the substituents of the molecules) or at least partially damaged (at least the functional group of the molecules is attacked). Because we find only 5−30% less "total C" from junctions prepared by direct evaporation than from surfaces without metal top contact, we conclude that most of the decomposition products of the molecules remain on the semiconductor surface.

4.3. Effect of Different Metals on the Electrical Characteristics of the Junctions. As shown in Figure 4, the $\ln(I)-V$ curves of Pd/dC-X/n-GaAs junctions are linear over a wider range (mostly between 0.1 and 0.6 V; actually linearity extends to 0.9 V for all curves) than those of the Au/dC-X/n-GaAs ones (mostly between 0.1 and 0.4 V). We ascribe this to differences in metal−semiconductor bonding details. For the molecularly modified samples, differences in metal−semiconductor bonding details occur because of varying degrees of metal penetration through pinholes and other defects in the monolayer. Based on the results reported in refs 66−68 we suggest that the lower reactivity of Au than of Pd with the GaAs surface[66] results in a higher density of electronic interface states for the Au−GaAs than for the Pd−GaAs contacts. The effect of such states on the $I-V$ characteristics increases as forward bias increases. Therefore, at higher forward bias the Au/GaAs $I-V$ characteristics are less regular than the Pd/GaAs ones.[55,67]

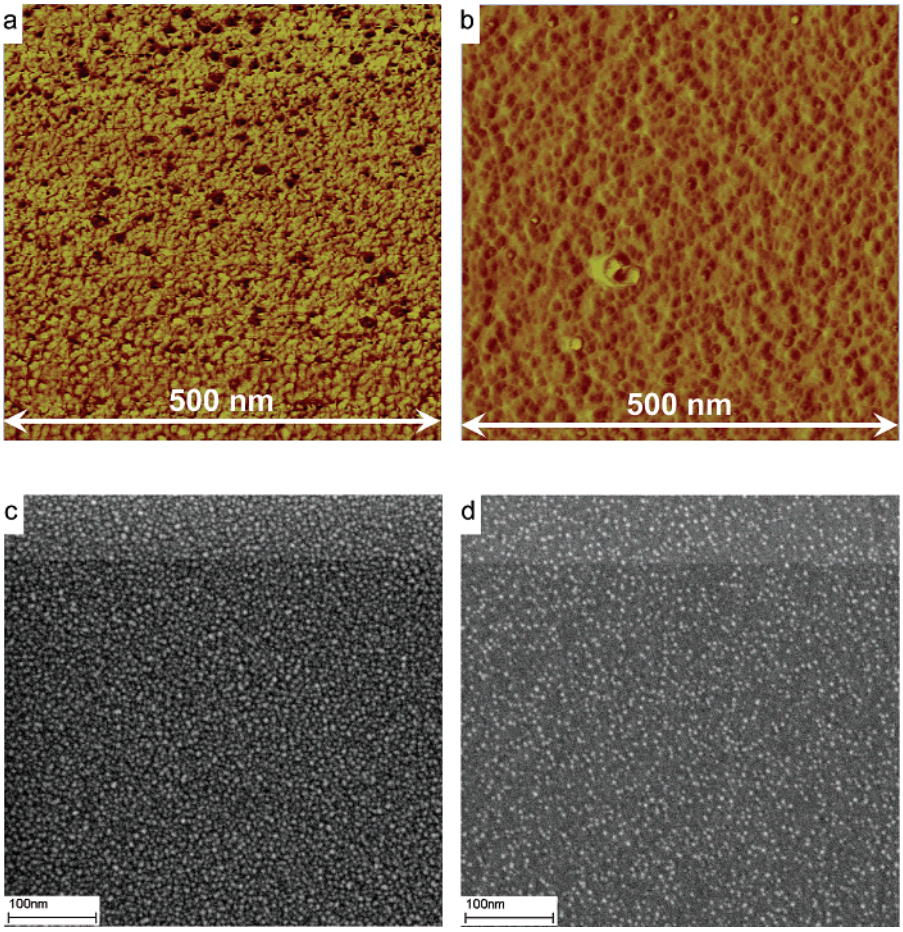

Figure 7. Top: AFM phase images of 1 nm nominal thickness of Au (a) and Pd (b) films deposited by indirect evaporation on dC-CF_3/GaAs surfaces. The color scale range is for (a) 25° and for (b) 10°. Bottom: Corresponding SEM images of the same Au (c) and Pd (d) films. The AFM and SEM images are shown at the same magnification.

Although the work functions of Pd and Au are very similar (~5 eV for both metals), there is a small but significant difference between the effective barrier height values of bare Pd/GaAs and Au/GaAs junctions prepared by indirect evaporation (Figure 6). This difference can be attributed to one of the following reasons or a combination of these:

(a) A higher density of pinning defects at the Au/n-GaAs interface than at the Pd/n-GaAs one.[68]

(b) A higher surface oxide concentration at the Au/n-GaAs interface than at the Pd/n-GaAs interface, because Au forms complexes with the oxide on GaAs while Pd reacts with the oxide and disperses it.[49,47,66] Angle-resolved XPS measurements of junctions formed by 1 nm Au on GaAs, prepared by indirect evaporation, showed GaAs−oxide "islands" up to 2−3 nm thick. Ellipsometry-based kinetic growth measurements showed that the GaAs−oxide layer forms after ~100 min exposure to ambient conditions,[49,40] which is the time delay between the end of the sample cleaning procedure and achieving 10^{-6} Torr vacuum pressure in the evaporator.

(c) Hydrogenation effects at the Pd/n-GaAs interface.[69,70] Hydrogen, from decomposition of H_2O molecules on the Pd surface, can diffuse through the metal bulk and accumulate at the Pd/GaAs interface. Such accumulation induces effective electrical charges/dipoles at the interface that decrease the effective work function of the Pd and, therefore, the barrier height of the Pd/n-GaAs junction. This effect will be absent at the Au/n-GaAs interface.

We ascribe the differences between BH values of bare junctions contacted by the same directly or indirectly deposited metal to the effects of radiation emitted from the metal source that arrives at the samples' surface during direct evaporation,[60] but not during indirect evaporation. Such radiation, which includes X-rays (as a result of electron−metal interaction) can be intense enough to lead to compositional changes of the GaAs surface[60] and can facilitate surface oxidation. Such oxidation decreases the negative charge on the GaAs surface and, thus, the band bending and Schottky barrier, compared to what is the case for junctions prepared with indirectly evaporated metal.

4.4. Why Do Junctions Contacted by Pd and Au Show Opposite Molecular Trends? The discussion of the results presented up to here does not explain the opposite trends of the barrier heights with electron affinity (CPD_L) between Au and Pd junctions made by indirect evaporation on the molecule-covered n-GaAs substrates (Figure 6). As the differences in damage observed by TOF SIMS for the dC-X molecules after Au and Pd evaporation are mostly within the experimental error (Table 2), this is unlikely to be the reason.

Experimentally we observe some morphological differences between the Au and Pd metal pads (cf. Figure 7), which we ascribe to how these films grow. Studies of the morphology of 1 nm nominal thickness (at larger thickness no clear differences can be seen) Au and Pd films by means of regular tapping mode AFM resulted in rather similar topographical images, but phase images (Figure 7a) combined with high-resolution SEM (Figure 7c) show that the Au film is much more textured and consists of separate particles rather than of a smooth film of metal. The phase image presented in Figure 7b shows that Pd covers the dC-CF_3/GaAs surface as a uniform layer, with some particulate

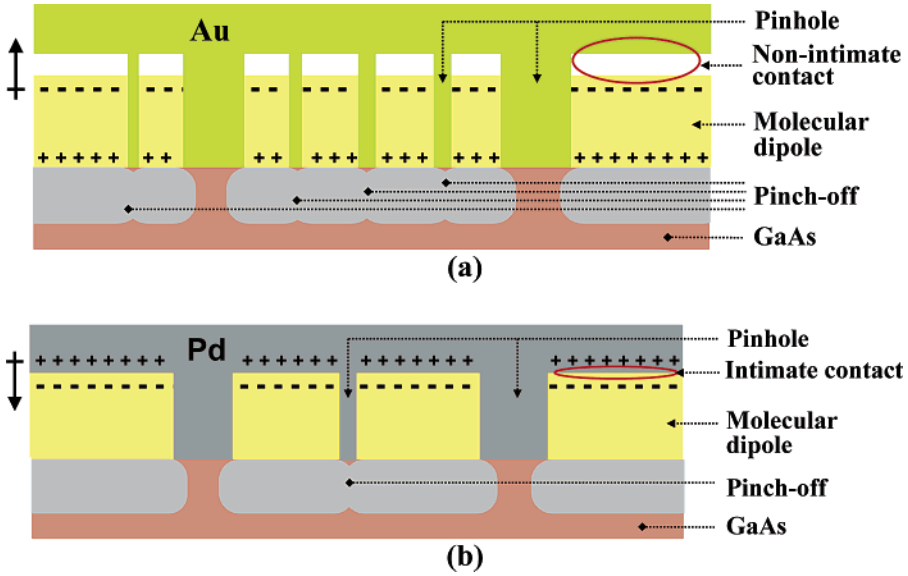

Figure 8. Simplified scheme of Pd and Au films, grown by indirect evaporation on molecularly modified surfaces.[47] In the case of (a) Au, 3-D growth dominates, while in the case of (b) Pd, growth is mostly 2-D. Molecular coverage on GaAs is generally 70−80% for dC-X[35] and 80−85% for BA-X molecules.[77] The dC-X thickness values, extracted from the capacitance data,[38] are 0.64−0.71 nm.[9,39,40]

islands of the next layer in the process of forming, as can be seen more clearly from the SEM image (Figure 7d), which offers higher resolution but not three-dimensionality. This evidence indicates the presence of different growth regimes of the two metals and results in different contact properties, as explained in the following two paragraphs.

While Pd grows in a two-dimensional (2-D) manner, Au growth is typically three-dimensional (3-D) because of its poor wetting properties (cf. Supporting Information, section 2).[47,71] Such 3-D growth will yield larger size clusters than the 2-D growth of Pd.[71,72] Pd forms a better covering layer than does Au, something that can be seen in Figure 7. The difference between junctions prepared with indirectly evaporated Au or Pd, shown in Figure 6, can be traced to differences in the metal/monolayer interface, in a manner analogous to our earlier explanation of differences between junctions with contacts prepared by two LOFO variants, one of which yields an intimate contact and one that yields a loose metal/molecule contact,[9] as will be explained now.

The preferred 2-D growth of Pd[47,71,73] will minimize Pd penetration through small defects in the dC-X monolayer. The preferred 3-D growth of Au will lead to accumulation of evaporated Au atoms and clusters in the monolayer pinholes. There they serve as the basis for 3-D growth,[47] and the end result is that the Au grows as clusters out of the pinholes, with voids between them, on top and over the molecular domains. In this scenario, the deposited Au does not yield an intimate contact with the molecules. Although formation of voids near pinholes in the monolayer cannot be excluded for evaporated Pd on dC-X/n-GaAs, this deposition is likely to form (mostly) intimate contact between the Pd and dC-X molecules.

In Figure 8, we show schematically junctions with indirectly evaporated Au or Pd on a molecular layer with an electron-withdrawing substituent group (e.g., CN or CF_3). Evidence for the net (relative) dipole direction comes from the experimentally determined direction of the change in barrier height, by assuming that this direction depends on the dipole of the molecules making up the layer (electron-withdrawing or electron-donating molecules; cf. ref 49). For Au, the direction of change fits with the dipole direction of the free molecule and that found for the molecular film on a free surface. For Pd the change in barrier height is opposite that expected from these directions. Within the above-mentioned assumption this means that with Au (Figure 8a) the poles of the dipole remain as in the free molecule, whereas with Pd (Figure 8b) the interaction between molecule and spillover electron density outside the metal surface inverts the interfacial dipole.[34,47] This effect is akin to what has also been termed the "pillow" effect.[74,75] Models for the (photo)-electrical behavior of inhomogeneous Schottky barriers were modified recently to discuss how this behavior is affected by charges in the monolayer for junctions contacted with Au (which forms a nonintimate contact) and Pd (which forms an intimate contact). For more details the reader is referred to refs 52 and 76.

To support this explanation, we prepared Au and Pd contacts on dC-X/n-GaAs surfaces by LOFO,[9] i.e., using "ready-made" pads to produce intimate electrical contact with the molecules. In that case, the same systematic molecular effect is obtained with both metals, as shown in their BH vs CPD_L plots, and is similar to that obtained with indirectly evaporated Pd junctions (Figure 9). These observations are consistent with those Pd junctions, but not the corresponding Au ones, forming intimate contact with the molecules.

The ranges of the molecular effects, in terms of difference between the highest and the lowest BHs, extracted for both types of LOFO-made junctions, were comparable (0.070 and 0.085 eV for Pd−LOFO and Au−LOFO, respectively). These values are significantly lower than those for junctions prepared by indirect evaporation. We can consider this difference in ranges by comparing the Pd-contacted junctions, as both the indirectly evaporated and LOFO-made ones show inversion of the free dipoles. The simplest explanation is then that the effective metal/molecule contact areas differ between the methods.[52] Complementary experiments showed indirectly evaporated contacts to have up to one order of magnitude larger effective contact areas than LOFO-made junctions (compare the data in Table 3 in ref 52). The larger the intimate contact area between deposited metal and molecules is, the higher the density of the inverted dipoles is, and the stronger will be the effect of these dipoles on the

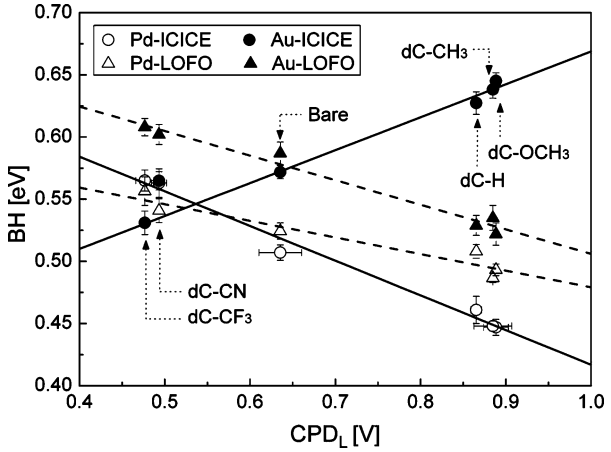

Figure 9. Dependence of effective barrier height (BH) of Pd/dC-X/n-GaAs junctions, contacted by indirect evaporation (ICICE) and lift-off, float-on (LOFO), on the CPD_L of the corresponding contact-free, molecularly modified n-GaAs surfaces. BH values for indirectly evaporated and LOFO-made junctions were calculated using data in the 0.06−0.40 V range. The difference in the BHs of the samples contacted by evaporation is explained in section 4.3. The higher BH values for LOFO-contacted junctions on bare samples, compared to those with evaporated contacts, can be attributed to the lower reactivity toward GaAs of the ready-made metal (LOFO) contact than of the evaporated one. Evaporated metals can react with oxides on GaAs,[81−83] while ready-made metal pads will be relatively inert. In such a case, current through LOFO-made junctions can encounter an additional oxide component of the barrier, leading to a higher effective BH compared to junctions contacted with evaporated contacts.

barrier height of the semiconducting substrate on which the molecules are adsorbed (cf. eq 1).

4.5. Effect of Metal Diffusion through the Molecular Films on the Junction Properties. The relation between device operation and Au diffusion through the molecular films was investigated by studying junctions on surfaces onto which, apart from the dC-X molecules, also a smaller molecule, benzoic acid (BA), was adsorbed. Earlier we showed that adsorption of substituted BA (BA-X) on n-GaAs yields a clear systematic change in CPD_L (cf. Table 3 and footnote *a* therein).[77] Molecular coverage on GaAs is generally 70−80% for dC-X[35] and 80−85% for BA-X molecules.[77] Together, the mixture of dC-X and BA-H yields a coverage of >95%.[78] It appears that BA-X molecules, with a footprint of ∼25 Å^2,[77] can fill pinholes with sizes smaller than the footprint of a dC-X molecule (∼40 Å^2),[36,79] consistent with our previous work on a hemin/benzoic acid mixture on GaAs(100).[80] Figure 10 shows how the BH for

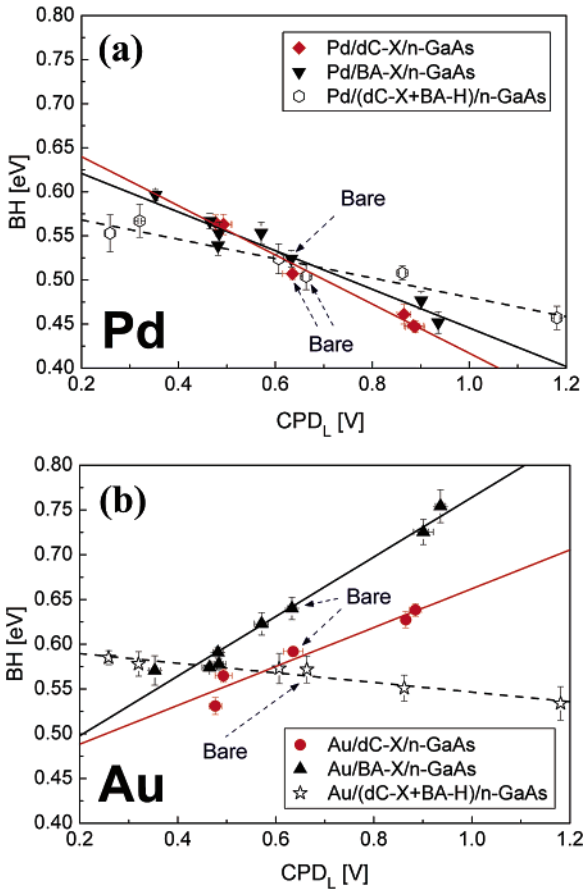

Figure 10. (a) Dependence of barrier height (BH) of Au/dC-X/n-GaAs, Au/BA-X/n-GaAs, and Au/(dC-X + BA-H)/n-GaAs junctions on the CPD_L of the corresponding contact-free monolayer/n-GaAs surfaces. (b) Dependence of BH of Pd/dC-X/n-GaAs, Pd/BA-X/n-GaAs, and Pd/(dC-X + BA-H)/n-GaAs junctions on the CPD_L of the corresponding contact-free monolayer/n-GaAs surfaces. For each series of junctions, a bare sample was prepared and measured. The differences between the data points for the bare (molecule-free) samples with the same metal contact are due to differences in oxides on the ambient-exposed GaAs substrate, which often make the bare samples the most difficult ones to measure (as dC-X and BA-H binding to such surfaces stabilizes them). The CPD_L values (and their errors) are given in Table 3.

different series of indirectly evaporated (Pd or Au) junctions on dC-X/n-GaAs, BA-X/n-GaAs, and (dC-X + BA-H)/n-GaAs surfaces depends on the CPD_L of the corresponding contact-free surfaces (cf. also Table 3). While the BH of the Au junctions

TABLE 3: Summary of the Measured CPD_L Values, the Surface Potential under Saturating GaAs Supra-Band-Gap Illumination (Corresponding to the Electron Affinity of the Surface, except for the 0.02 eV Energy Difference between the Fermi Level and Conduction Band) for n-GaAs Surfaces onto Which the Dicarboxylic or Benzoic Acid Derivatives, dC-X and BA-X, Respectively, Were Adsorbed

benzoic acid (BA-X)		dicarboxylic acid (dC-X)		mixture of dC-X and BA-H	
X	CPD_L[a] (V)	X	CPD_L (V)	X	CPD_L (V)
$-N(CH_3)_2$	0.94 ± 0.02	$-OCH_3$	0.89 ± 0.02	$-OCH_3$	1.18 ± 0.04
$-OCH_3$	0.90 ± 0.02	$-CH_3$	0.89 ± 0.040	$-CH_3$	0.61 ± 0.03
bare	0.63 ± 0.03	−H	0.87 ± 0.02	−H	0.86 ± 0.03
−H	0.57 ± 0.02	bare	0.64 ± 0.03	bare	0.67 ± 0.03
−F	0.47 ± 0.01	$-CF_3$	0.50 ± 0.02	$-CF_3$	0.32 ± 0.02
−Br	0.48 ± 0.02	−CN	0.48 ± 0.02	−CN	0.26 ± 0.02
$-CF_3$	0.35 ± 0.03				
$-NO_2$	0.35 ± 0.02				
−CN	0.48 ± 0.02				

[a] Converting the obtained CPD_L to electron affinity (χ) values and comparing them to results from our earlier report,[77] for similar molecularly modified surfaces, shows deviations between −5 and +5%. These deviations can be attributed to different concentrations of GaAs−oxide, Ga, or As, due to the different procedures used to etch the GaAs surfaces. While in ref 77 we used 0.05% (v/v) Br_2/MeOH and 1 M KOH(aq) to etch the substrates, here we used $NH_4OH:H_2O$ (1:10 v/v) solution.

made with dC-X and BA-X layers *increases* as a function of CPD_L, for Au junctions with (dC-X + BA-H) it slightly *decreases* (Figure 10b). The trend for the Au junctions with the mixture of molecules is weaker than for that of Pd and much smaller than for the junctions of Pd on/dC-X or on BA-X layers (cf. Figure 10a). The differences between these results are likely due to the effect of pinholes, as explained below.

In section 4.4 we argued that the intimate contact of Pd with the molecules inverts the dipoles of the adsorbed dC-X molecules. Therefore, it yields a BH trend opposite that obtained with a nonintimate contact, such as that formed by indirectly evaporated Au, where the dipole direction of one molecule relative to another remains as on the free, molecularly modified surface.[34,47]

Increasing the fraction of the surface covered by molecules, by coadsorbing BA-H molecules, should decrease the probability of Au penetration into the pinholes. In this way (direct) Au growth on top of the molecular domains is expected to be the dominant process, resulting in a more intimate contact between Au and the mixture of molecules. This type of contact will reverse the trend of the BH, as compared to what is the case for Au/dC-X/n-GaAs junctions, where the Au forms mostly nonintimate contact with the molecular domains.

The range of BH values, which we can express as $|\gamma| = |\Delta BH/\Delta CPD_L|$, is much smaller for Au/(dC-X + BA-H)/n-GaAs (0.06 eV/V) than for Au/dC-X/n-GaAs (0.30 eV/V). We suggest that this is due to partial cancellation of dipole effects. Such a cancellation can occur because there will be more intimate metal/molecule contacts with the mixed (dC-X + BA-H) layer, where the dipole effect is reversed, than with the pure dC-X parts of the layer. Another reason for the low $|\gamma|$ value is that there is likely to be some overgrowth of the metal over the shorter BA-H domains that are expected to exist within the dC-X domains. This latter factor also explains the lower $|\gamma|$ value for Pd/(dC-X + BA-H)/n-GaAs than that for the analogous junctions with dC-X or BA-H (cf. Figure 10a).

4.6. Effect of Different Metals on the Molecules during Direct Evaporation. Although direct evaporation of Pd and Au yielded no trends of BH vs molecular parameters, the ln(I)−V curves (Figure 5) and the TOF SIMS results (Table 2) indicate that some differences exist between directly evaporated Au and Pd. The TOF SIMS results show that with directly evaporated Pd junctions twice as many binding groups are preserved, but damage to the functional CF_3 group is 30% more severe than with the corresponding Au ones. This may explain why all dC-X-modified GaAs surfaces contacted with Pd show similar $I-V$ behavior (as the functional group that differentiates between molecules is more affected than if Au is directly evaporated), while for Au this is less so.

5. Conclusions

From our experimental observations we deduce that contacting molecules by direct evaporation can affect them in a number of ways: (I) metal penetration through pinholes; (II) metal penetration between the chains of the molecules; (III) total damage to the molecules, so that the decomposed residues are removed from the surface; (IV) total damage to the molecules, so that the molecular residues remain in part or fully on the surface (cooling the substrate increases this possibility); (V) partial damage to the molecules, so that at least their functional groups are damaged; and (VI) contacting the molecules without damaging either their ligands or their functional groups.

Metal/molecule/semiconductor junctions are found to constitute a sensitive tool to estimate damage. In all cases (I) will be present. For direct evaporation this will also include (III). For Au we assume also (II) to occur. The TOF SIMS and XPS results can then be interpreted to show that the current−voltage characteristics of the Pd/dC-X/n-GaAs junction made by direct evaporation will be an average of the characteristics of mostly decomposed/damaged molecules (i.e., scenarios IV and/or V) and of a minority of undamaged molecules (i.e., scenario VI), while those of the indirectly evaporated ones will be the opposite.

In agreement with earlier results of ours,[9,33,34] we find that details of the metal contacting procedures can completely change resulting electronic device characteristics. In the case of metal evaporation even experiments that use cooled substrates should be viewed with caution also if they do not show device shorting, a*s this cannot ensure that the molecules have not been damaged*. Rather, unless evidence to the contrary is available, it is likely that the measured electrical characteristics represent an average of damaged as well as undamaged molecules. Indirect evaporation of metal on a cooled substrate minimizes damage to molecules sufficiently so that molecular trends due to the part of the molecule that is most exposed to the evaporation process are preserved in the resulting devices. Evaporation of Pd is to be preferred over Au, because of its 2-D growth mechanism, which limits its interaction with the molecules to the outer end, onto which the metal is deposited.

Acknowledgment. D.C. thanks the Israel Science Foundation, the Minerva Foundation, and the Grand Centre for Sensors and Security for partial support. We thank Prof. A. Shanzer for continuing collaboration and Ms. R. Lazar for skillful technical assistance with the syntheses of the dC-X molecules. We acknowledge fruitful discussions with Drs. M. Ambrico and T. Ligonzo (Bari, Italy). D.C. holds the Schaefer chair in energy research.

Supporting Information Available: Wetting properties of Pd and Au during film formation on (solid) substrates. This material is available free of charge via the Internet at http://pubs.acs.org.

References and Notes

(1) Tour, J. M. *Acc. Chem. Res.* **2000**, *33*, 791.
(2) Ashkenasy, G.; Cahen, D.; Cohen, R.; Shanzer, A.; Vilan, A. *Acc. Chem. Res.* **2002**, *35*, 121.
(3) Gates, B. D.; Xu, Q.; Stewart, M.; Ryan, D.; Willson, C. G.; Whitesides, G. M. *Chem. Rev.* **2005**, *105*, 1171.
(4) Aviram, A.; Ratner, M. *Molecular electronics: science and technology, 1998*; Annals of the New York Academy of Sciences 852; New York Academy of Sciences: New York, 1998.
(5) Hsu, J. W. P. *Mater. Today* **2005**, *8*, 42.
(6) Cui, X. D.; Zarate, X.; Tomfohr, J.; Sankey, O. F.; Primak, A.; Moore, A. L.; Moore, T. A.; Gust, D.; Harris, G.; Lindsay, S. M. *Nanotechnology* **2002**, *13*, 5.
(7) Cahen, D.; Hodes, G. *Adv. Mater.* **2002**, *14*, 789.
(8) Rampi, M. A.; Whitesides, G. M. *Chem. Phys.* **2002**, *281*, 373.
(9) Vilan, A.; Cahen, D. *Adv. Funct. Mater.* **2002**, *12*, 795.
(10) Shimizu, K. T.; Fabbri, J. D.; Jelincic, J. J.; Melosh, N. A. *Adv. Mater.* **2006**, *18*, 1499.
(11) Loo, Y.-L.; Willett, R. L.; Baldwin, K. W.; Rogers, J. A. *J. Am. Chem. Soc.* **2002**, *124*, 7654.
(12) Xia, Y.; Whitesides, G. M. *Annu. Rev. Mater. Sci.* **1998**, *28*, 153.
(13) Hrapovic, S.; Liu, Y.; Enright, G.; Bensebaa, F.; Luong, J. H. T. *Langmuir* **2003**, *19*, 3958.
(14) Kushmerick, J. G.; Holt, D. B.; Yang, J. C.; Naciri, J.; Moore, M. H.; Shashidhar, R. *Phys. Rev. Lett.* **2002**, *89*, 086802/1.
(15) Slowinski, K.; Fong, H. K. Y.; Majda, M. *J. Am. Chem. Soc.* **1999**, *121*, 7257.
(16) Kruger, J.; Bach, U.; Gratzel, M. *Adv. Mater.* **2000**, *12*, 447.
(17) Akkerman, H. B.; Blom, P. W. M.; de Leeuw, D. M.; de Boer, B. *Nature* **2006**, *441*.
(18) Beebe, J. M.; Engelkes, V. B.; Miller, L. L.; Frisbie, C. D. *J. Am. Chem. Soc.* **2002**, *124*, 11268.
(19) Zhou, C.; Muller, C. J.; Deshpande, M. R.; Sleight, J. W.; Reed, M. A. *Appl. Phys. Lett.* **1995**, *67*, 1160.

(20) Zhou, C.; Deshpande, M. R.; Reed, M. A.; Jones, K., II; Tour, J. M. *Appl. Phys. Lett.* **1997**, *71*, 611.
(21) Lioubtchenko, D. V.; Markov, I. A.; Briantseva, T. A. *Appl. Phys. Lett.* **2003**, *211*, 335.
(22) Haynie, B. C.; Walker, A. V.; Tighe, T. B.; Allara, D. L.; Winograd, N. *Appl. Surf. Sci.* **2003**, *203*−*204*, 433.
(23) de Boer, B.; Frank, M. M.; Chabal, Y. J.; Jiang, W.; Garfunkel, E.; Bao, Z. *Langmuir* **2004**, *20*, 1539.
(24) Ohgi, T.; Sheng, H.-Y.; Dong, Z.-C.; Nejoh, H. *Surf. Sci.* **1999**, *422*, 277.
(25) Jung, D. R.; Czanderna, A. W.; Herdt, G. C. *J. Vac. Sci. Technol., A* **1996**, *14*, 1779.
(26) Zahl, H. A.; Golay, M. J. E. *Rev. Sci. Instrum.* **1946**, *17*, 511.
(27) Lee, J.-O.; Lientschnig, G.; Wiertz, F.; Struijk, M.; Janssen, R. A. J.; Egberink, R.; Reinhoudt, D.; Hadley, P.; Dekker, C. *Nano Lett.* **2003**, *3*, 113.
(28) Okazaki, N.; Sambles, J. R. *International Symposium on Organic Molecular Electronics*, Nagoya, Japan, 2000; pp 66−67.
(29) Fisher, G. L.; Walker, A. V.; Hooper, A. E.; Tighe, T. B.; Bahnck, K. B.; Skriba, H. T.; Reinard, M. D.; Haynie, B. C.; Opila, R. L.; Winograd, N.; Allara, D. L. *J. Am. Chem. Soc.* **2002**, *124*, 5528.
(30) Hooper, A.; Fisher, G. L.; Konstadinidis, K.; Jung, D.; Nguyen, H.; Opila, R.; Collins, R. W.; Winograd, N.; Allara, D. L. *J. Am. Chem. Soc.* **1999**, *121*, 8052.
(31) Jun, Y.; Zhu, X.-Y.; Hsu, J. W. P. *Langmuir* **2006**, *22*, 3627.
(32) Aswal, D. K.; Lenfant, S.; Guerin, D.; Yakhmi, J. V.; Vuillaume, D. *Small* **2005**, *1*, 725.
(33) Haick, H.; Ambrico, M.; Ghabboun, J.; Ligonzo, T.; Cahen, D. *Phys. Chem. Chem. Phys.* **2004**, *6*, 4538.
(34) Haick, H.; Ghabboun, J.; Cahen, D. *Appl. Phys. Lett.* **2005**, *86*, 042113/1.
(35) Haick, H.; Ambrico, M.; Ligonzo, T.; Cahen, D. *Adv. Mater.* **2004**, *16*, 2145.
(36) Cohen, R.; Kronik, L.; Shanzer, A.; Cahen, D.; Liu, A.; Rosenwaks, Y.; Lorenz, J. K.; Ellis, A. B. *J. Am. Chem. Soc.* **1999**, *121*, 10545.
(37) Vilan, A.; Ussyshkin, R.; Gartsman, K.; Cahen, D.; Naaman, R.; Shanzer, A. *J. Phys. Chem. B* **1998**, *102*, 3307.
(38) Yu, H.-Z.; Morin, S.; Wayner, D. D. M.; Allongue, P.; Henry de Villeneuve, C. *J. Phys. Chem. B* **2000**, *104*, 11157.
(39) Iozzi, M. F.; Cossi, M. *J. Phys. Chem. B* **2005**, *109*, 15383.
(40) Vilan, A. Ph.D. Thesis, Weizmann Institute of Science, 2002.
(41) We use here as the relevant dipole moment that of the molecule bound to the GaAs surface, as calculated in ref 39, rather than the free molecule's dipole moment, as we did in earlier work. We note that, as noted also in ref 47, the general trends are very similar, reflecting the changes within the series of molecules with identical binding group.
(42) Moench, W. *Semiconductor surfaces and interfaces*, 3rd revised ed.; Springer-Verlag: Berlin, Germany, 2001.
(43) Evans, S. D.; Ulman, A. *Chem. Phys. Lett.* **1990**, *170*, 462.
(44) Bruening, M.; Moons, E.; Cahen, D.; Shanzer, A. *J. Phys. Chem.* **1995**, *99*, 8368.
(45) Gershevitz, O.; Sukenik, C. N.; Ghabboun, J.; Cahen, D. *J. Am. Chem. Soc.* **2003**, *125*, 4730.
(46) Frisch, M. J.; Trucks, G. W.; Schlegel, H. B.; Scuseria, G. E.; Robb, M. A.; Cheeseman, J. R.; Montgomery, J. A., Jr.; Vreven, T.; Kudin, K. N.; Burant, J. C.; Millam, J. M.; Iyengar, S. S.; Tomasi, J.; Barone, V.; Mennucci, B.; Cossi, M.; Scalmani, G.; Rega, N.; Petersson, G. A.; Nakatsuji, H.; Hada, M.; Ehara, M.; Toyota, K.; Fukuda, R.; Hasegawa, J.; Ishida, M.; Nakajima, T.; Honda, Y.; Kitao, O.; Nakai, H.; Klene, M.; Li, X.; Knox, J. E.; Hratchian, H. P.; Cross, J. B.; Bakken, V.; Adamo, C.; Jaramillo, J.; Gomperts, R.; Stratmann, R. E.; Yazyev, O.; Austin, A. J.; Cammi, R.; Pomelli, C.; Ochterski, J. W.; Ayala, P. Y.; Morokuma, K.; Voth, G. A.; Salvador, P.; Dannenberg, J. J.; Zakrzewski, V. G.; Dapprich, S.; Daniels, A. D.; Strain, M. C.; Farkas, O.; Malick, D. K.; Rabuck, A. D.; Raghavachari, K.; Foresman, J. B.; Ortiz, J. V.; Cui, Q.; Baboul, A. G.; Clifford, S.; Cioslowski, J.; Stefanov, B. B.; Liu, G.; Liashenko, A.; Piskorz, P.; Komaromi, I.; Martin, R. L.; Fox, D. J. K., T.; Al-Laham, M. A.; Peng, C. Y.; Nanayakkara, A.; Challacombe, M.; Gill, P. M. W.; Johnson, B.; Chen, W.; Wong, M. W.; Gonzalez, C.; Pople, J. A. *Gaussian 03*, revision C.02; Gaussian, Inc.: Wallingford, CT, 2004.
(47) Haick, H.; Ghabboun, J.; Niitsoo, O.; Cohen, H.; Cahen, D.; Vilan, A.; Hwang, J.; Wan, A.; Amy, F.; Kahn, A. *J. Phys. Chem. B* **2005**, *109*, 9622.
(48) Vilan, A.; Shanzer, A.; Cahen, D. *Nature* **2000**, *404*, 166.
(49) Vilan, A.; Ghabboun, J.; Cahen, D. *J. Phys. Chem. B* **2003**, *107*, 6360.
(50) Salomon, A.; Berkovich, D.; Cahen, D. *Appl. Phys. Lett.* **2003**, *82*, 1051.
(51) Rhoderick, E. H. *Metal-semiconductor contacts*; Oxford University Press: London, U.K., 1978.
(52) Haick, H.; Ambrico, M.; Ligonzo, T.; Tung, R. T.; Cahen, D. *J. Am. Chem. Soc.* **2006**, *128*, 6854.
(53) Kronik, L.; Shapira, Y. *Surf. Sci. Rep.* **1999**, *37*, 1.
(54) The direction of the molecular dipole is positive if the negative pole of the dipole points away from the binding group, viz. away from the surface after binding.
(55) Tung, R. T. *Mater. Sci. Eng., R: Rep.* **2001**, *R35*, 1.
(56) The ideality factor $n = 1$ for an ideal Schottky barrier. For many rectifying junctions it can be determined empirically by fitting the functional form of the experimentally observed currents (eq 1). All other factors being equal, the higher the n values are the higher the Schottky barrier height variation is, i.e., the larger the degree of inhomogeneity of the junction is.
(57) Schwieters, J.; Cramer, H. G.; Heller, T.; Juergens, U.; Niehuis, E.; Zehnpfenning, J.; Benninghoven, A. *J. Vac. Sci. Technol.* **1991**, *9*, 2864.
(58) Weissler, G. L.; Carlson, R. W. *Methods of experimental physics*; Academic Press: New York, 1979; Vol. 14.
(59) This does not exclude physisorption of gaseous monolayers (e.g., of O_2, N_2, or H_2O) on the substrate, especially on a cooled substrate. At room temperature and vacuum between 10^{-4} and 10^{-7} mbar, a monolayer of gaseous O_2 or N_2 forms on the substrate after ca. 0.02 or 20 s, respectively.
(60) Lioubtchenko, D. V.; Markov, I. A.; Briantseva, T. A. *Appl. Surf. Sci.* **2002**, *195*, 42.
(61) Molvik, A. W.; Covo, M. K.; Bieniosek, F. M.; Prost, L.; Seidl, P. A.; Baca, D.; Coorey, A.; Sakumi, A. *Phys. Rev. Spec. Top.—Accel. Beams* **2004**, *7*, 093202.
(62) Using a gas with higher atomic weight (Xe or inert molecules with higher molecular weight), instead of Ar is more effective, but it is more expensive and can complicate the system.
(63) Ulman, A. *Chem. Rev.* **1996**, *96*, 1533.
(64) Dubois, L. H.; Nuzzo, R. G. *Annu. Rev. Phys. Chem.* **1992**, *43*, 437.
(65) Love, J. C.; Estroff, L. A.; Kriebel, J. K.; Nuzzo, R. G.; Whitesides, G. M. *Chem. Rev.* **2005**, *105*, 1103.
(66) Yablonovitch, E.; Sands, T.; Hwang, D. M.; Schnitzer, I.; Gmitter, T. J.; Shastry, S. K.; Hill, D. S.; Fan, J. C. C. *Appl. Phys. Lett.* **1991**, *59*, 3159.
(67) Heslinga, D. R.; Weitering, H. H.; Van der Werf, D. P.; Klapwijk, T. M.; Hibma, T. *Phys. Rev. Lett.* **1990**, *64*, 1589.
(68) Drummond, T. J. *Phys. Rev. B* **1999**, *59*, 8182.
(69) Nie, H. Y.; Nannichi, Y. *Jpn. J. Appl. Phys., Part 1* **1991**, *30*, 906.
(70) Nie, H. Y.; Nannichi, Y. *Jpn. J. Appl. Phys., Part 2* **1993**, *32*, L890.
(71) Li, Y.; DePristo. *Surf. Sci.* **1996**, *351*, 189.
(72) Schmidt, A. A.; Eggers, H.; Herwig, K.; Anton, R. *Surf. Sci.* **1996**, *349*, 301.
(73) Metal condensation from the gas phase involves nucleation of dense particle clusters, particle growth kinetics, and film formation by coalescence. For metals such as Au, nucleation is relatively poor, which leads initially to growth of a limited number of clusters (i.e., 3-D growth). In contrast, with Pd, where nucleation is favorable, many clusters will form, grow, and quickly coalesce into a continuous film (i.e., 2-D growth). The reason is that kinks at the edges of growing Pd islands decrease the (potential energy) barriers for atoms to reach the edge 2−3-fold, relative to what is the case for Au. As a result, the probability for an atom, landing on top of a growing metal island, to reach the island's edge before another adatom lands on the same island is significantly higher for Pd than for Au. Because of this and since both metals have similar cohesive energies (3.9 and 3.8 eV for Pd and Au, respectively), formation of a continuous Au film will require thicker coverage than for Pd and, thus, will take longer.
(74) Ishii, H.; Sugiyama, H.; Ito, E.; Seki, K. *Adv. Mater.* **1999**, *11*, 605.
(75) Vazquez, H.; Gao, W.; Flores, F.; Kahn, A. *Phys. Rev. B* **2005**, *71*, 041306/1.
(76) Haick, H.; Pelz, J. P.; Ligonzo, T.; Ambrico, M.; Cahen, D.; Cai, W.; Marginean, C.; Tivarus, C.; Tung, R. T. *Phys. Status Solidi A* **2006**, *203*, 3438.
(77) Bastide, S.; Butruille, R.; Cahen, D.; Dutta, A.; Libman, J.; Shanzer, A.; Sun, L.; Vilan, A. *J. Phys. Chem. B* **1997**, *101*, 2678.
(78) Coverage was estimated using a combination of several characterization techniques, viz., Kelvin probe, ellipsometry and contact angle measurements, and Fourier transform infrared spectroscopy.
(79) dC-X molecules have "bulky" shapes and a surface area of ca. 40 $Å^2$/molecule, whereas BA molecules are more linear with smaller surface area (~25 $Å^2$/molecule). It is therefore likely that BA can form more dense molecular domains than dC-X and, thus, induce (on the average) stronger electrostatic effects.
(80) Wu, D. G.; Cahen, D.; Graf, P.; Naaman, R.; Nitzan, A.; Shvarts, D. *Chem.—Eur. J.* **2001**, *7*, 1743.
(81) Weizer, V. G.; Fatemi, N. S. *J. Appl. Phys.* **1988**, *64*, 4618.
(82) Persson, A. I.; Larsson, M. W.; Stenstroem, S.; Ohlsson, B. J.; Samuelson, L.; Wallenberg, L. R. *Nat. Mater.* **2004**, *3*, 677.
(83) Gupta, R. P.; Khokle, W. S.; Wuerfl, J.; Hartnagel, H. L. *Thin Solid Films* **1987**, *151*, L121.